Pragmatic phase noise compensation for high-order coded modulations

Marco Martalò[1,2] ✉, Gianluigi Ferrari[1], Muhammad Asim[1], Jonathan Gambini[3], Christian Mazzucco[3], Giacomo Cannalire[3], Sergio Bianchi[3], Riccardo Raheli[1]

[1]Department of Information Engineering, University of Parma, Italy
[2]E-Campus University, Novedrate (CO), Italy
[3]European Research Center, Huawei Technologies, Milan, Italy
✉ E-mail: marco.martalo@unipr.it

Abstract: This study discusses synchronisation in phase noise-impaired spectrally efficient communication systems employing high-order modulations. In particular, an iterative receiver, where demodulation and decoding are separate from maximum a posteriori probability (MAP) synchronisation, is presented. The authors' separate approach is tailored to the design of pragmatic iterative receiver schemes employing 'off-the-shelf' demodulation and decoding blocks. This allows full compatibility with already existing systems, which is attractive from the implementation viewpoint. The proposed MAP synchronisation algorithm also requires very limited knowledge of the phase noise process and achieves near coherent performance with moderate computational complexity. Although the approach is very general, the authors discuss its performance for low-density parity-check-coded pilot symbol-aided quadrature amplitude modulation schemes, demonstrating that a significantly lower computational complexity can be achieved with respect to benchmark joint receivers.

1 Introduction

Wireless and optical communication systems employ oscillators to generate signals used for frequency conversions and synchronisation purposes. Oscillators should generate ideal sinusoidal waveforms, but in practice they are subject to noise, i.e. temporal instabilities and spectral dispersions, which are detrimental for the performance of communication systems. In fact, this noise may cause signal distortion, information loss, and high bit error rate (BER). The noise in the waveform generated by a realistic oscillator is denoted as phase noise [1] and it is a well-known topic in the literature. From an information-theoretic perspective, the ultimate performance in the presence of phase noise has been studied in terms of the achievable information rate under several channel models [2–5].

The impact of phase noise on the performance of communication systems has been also studied from the receiver design viewpoint. In [6], the authors consider the use of a turbo code and design an iterative receiver based on phase discretisation, showing also that the phase can be effectively estimated only by the first component decoder. Another approach, reviewed in [7], is based on an iterative maximum likelihood (ML) algorithm used in an expectation-maximisation (EM) receiver. This approach can be denoted as *separate*, since detection/decoding is performed separately from phase synchronisation. Extensions to iterative phase locked loop (PLL)-based schemes are proposed in [8–10], but are tailored for specific coded modulation schemes with small size constellations. Variational Bayesian detection with a proper phase noise model is proposed in [11], in which, as an alternative approach, synchronisation and decoding are performed *jointly*. In [12], the authors exploit the phase error statistics to devise an ML detector and related suboptimal versions based on approximations of the probability density function (PDF) of the phase error. In [13], a Gaussian sum approach is proposed to derive a phase estimation and tracking algorithm in a blind context, i.e. a scenario where no initial phase knowledge is available to eliminate ambiguities. A maximum a posteriori probability (MAP)-based

soft-input soft-output (SISO) decoder for a specific case study with 8-phase shift keying (PSK) modulation and turbo coding related to the solution here presented has been brought to our attention after the conclusion of this work [14]. To the best of our knowledge, a benchmark joint solution is proposed in [15], where a suitable factor graph, modelling both the channel code and the phase noise process, is considered for the maximisation of the a posteriori probabilities (APPs) of the information symbols. Therefore, [15] will be considered as the reference algorithm for phase noise compensation in the remainder of this paper.

We derive a MAP phase estimation algorithm, which is then employed in an efficient iterative receiver, where demodulation and decoding operations are separated from the synchronisation. This allows the design of an effective pragmatic receiver for large constellation sizes, which are a key tool to achieve high spectral efficiencies in modern communication systems. The devised algorithm has the key advantage that it does not depend on the considered modulation/coding scheme and requires very limited statistical knowledge of the phase noise process. In fact, in order to keep the computational complexity as low as possible, we first assume that the phase noise is approximately constant over a (sufficiently short) interval. The resulting phase estimation strategy is referred to as block window (BW). The assumption of constant phase noise is then relaxed by employing a sliding window to smooth the piecewise estimation of the BW method; this approach will be referred to as phasor linear prediction (PLP), due to similarities with the phase estimation approach proposed in [16].

Despite the proposed approach is very general, as a representative case study we consider low-density parity-check (LDPC)-coded quadrature amplitude modulation (QAM) schemes. The results of our analysis show very good performance for medium–high constellation sizes and relatively strong phase noise. The proposed receiver exhibits an appreciably lower computational complexity with respect to the joint approach in [15], at the cost of a minor performance degradation. This paper expands upon a preliminary conference version [17].

The rest of the paper is structured as follows. In Section 2, the system model is presented. In Section 3, the proposed APP-based synchronisation algorithm is derived. In Section 4, the corresponding iterative receiver is shown. In Section 5, numerical results are presented. In Section 6, computational complexity considerations are presented. Finally, Section 7 provides concluding remarks.

2 System model

Fig. 1 shows the considered system model. A binary information sequence $\{a_i\}$ is encoded into a sequence $\{c_j\}$ by a rate-R channel code. A modulation with constellation set $\mathcal{X}$ of size $M = 2^b$, where b is the number of bits per symbol and average symbol energy E_s is employed. Spectrally efficient modulations are obtained by means of multi-level coding (MLC) schemes [18]. The following MLC strategy is considered:

• For small constellation sizes, i.e. $b \leq b_1$, where b_1 is a small positive integer, all bits are channel encoded. Therefore, the spectral efficiency is $\eta = Rb$ bits per symbol.
• For larger constellation sizes, i.e. for $b > b_1$, b_1 bits are channel encoded and $b - b_1$ are left uncoded (free bits). In particular, the channel encoded bits identify one of 2^{b_1} possible subsets in a constellation with $M = 2^b$ points. The free bits, instead, label the points of the selected subset using Gray mapping [19, 20]. According to Ungerboeck set partitioning [21], subsets are designed so that the Euclidean distance is maximised. In this case, the spectral efficiency is $\eta = R \cdot b_1 + (b - b_1)$ bits per symbol.

The derived iterative receiver is independent of the specific coded modulation scheme. However, in Section 5 we focus on LDPC-coded M-QAM schemes and, in particular, we set $b_1 = 4$, i.e. all bits are channel coded up to 16-QAM.

Coarse initial synchronisation is needed to bootstrap the receiver in the absence of the APPs on the transmitted symbols. To this end, we use, at known time instants, pilot symbols, whose values are perfectly known at the receiver [22]. In particular, N_p pilot symbols, with energy E_p each, are inserted every N data symbols. The average energy per information data symbol can then be expressed as

$$\overline{E}_s = \frac{N_p E_p + N E_s}{N} = E_s(1 + q)$$

where

$$q \triangleq \frac{N_p E_p}{N E_s}.$$

The energy penalty caused by pilot symbols is described by factor $(1 + q)$. In Section 4, we provide details on the use of pilot symbols at the receiver.

The continuous-time channel introduces AWGN and phase noise. For sufficiently low phase noise intensity [4], the discrete-time observable at the output of a receiver matched filter can be expressed as

$$r_k = x_k e^{j\theta_k} + n_k \quad k = 0, 1, 2, \ldots \tag{1}$$

where $\{x_k\}$ are the transmitted symbols and $\{n_k\}$ are independent and identically distributed (i.i.d.) Gaussian noise complex samples with per-component variance $\sigma^2 = N_0/2$. The per-bit signal-to-noise ratio (SNR) γ_b can be defined as follows

$$\gamma_b \triangleq \frac{E_b}{N_0} = \frac{\overline{E}_s}{N_0} \frac{1}{\eta} = \frac{E_s}{N_0} \frac{1 + q}{\eta}.$$

The discrete-time model of phase noise considered in this paper is the well-known Wiener model used in most of the literature [1–6, 23]

$$\theta_k = \theta_{k-1} + \sigma_\Delta w_k \quad k = 0, 1, 2, \ldots \tag{2}$$

where $w_k \sim \mathcal{N}(0, 1)$ are i.i.d. zero mean and unit-variance Gaussian increments, σ_Δ is a system parameter characterising the phase noise intensity and θ_{-1} is an initial phase uniformly distributed in $[0, 2\pi)$. This model is representative (in discrete time) of the experimental (continuous) time-varying phase noise process affecting local oscillators, which exhibits a quadratic power spectrum decay [24]. We, however, remark that the proposed APP-based iterative synchronisation algorithm requires very limited a priori information on the phase noise statistical characterisation, as will be discussed in Section 4. Therefore, it can be directly applied to other (more complex) models found in the literature [25, 26].

The principle of the iterative receiver, shown in Fig. 1, is based on two separate blocks, which perform SISO demodulation/decoding and phase estimation, and iteratively exchange their own information. In particular, phase estimation, which will be described in Section 3, exploits the symbol APPs output by a standard off-the-shelf SISO decoder. On the other hand, the phase estimates are used by the demodulation/decoding block to compensate and 'clean' the received observable. The complete iterative receiver structure is detailed in Section 4.

3 APP-based phase synchronisation

Accurate symbol-by-symbol phase tracking typically requires large computational complexity, especially in schemes employing high-order coded modulations. In order to reduce the computational complexity of the phase estimation algorithm, we first approximate the channel phase noise as constant over a (sufficiently short) observation window composed by ℓ consecutive samples. This means that we perform block-wise phase noise estimation. In fact, the phase estimate on a length-ℓ block is used to compensate for the phase rotations over all symbols of the same block. Moreover, phase estimates of consecutive blocks will differ from each other. This window length ℓ is a compromise system parameter which needs to be properly chosen. In fact, a small value of ℓ is desirable to make the assumption of constant phase noise realistic; on the other hand,
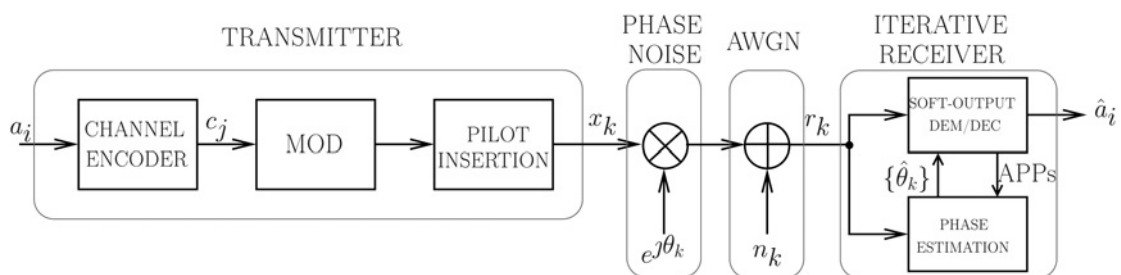

Fig. 1 *System model and principle of the iterative receiver*

a large value of ℓ may be useful to average the detrimental effects of AWGN.

In Section 3.1, we first focus on disjoint consecutive windows leading to the BW approach. Then, in Section 3.2 a sliding window strategy, referred to as PLP, is also derived as an extension of the BW approach.

3.1 Block window

Let us define the following vector of observables associated with a length-ℓ window starting at the kth epoch

$$\boldsymbol{r}_k \triangleq [r_k, r_{k+1}, \ldots, r_{k+\ell-1}] \quad k = 0, 1, \ldots$$

Therefore, the entire sequence of received samples in the same codeword is composed by some number n_p of disjoint blocks, i.e.

$$\boldsymbol{r} = [\boldsymbol{r}_0, \boldsymbol{r}_\ell, \ldots, \boldsymbol{r}_{(n_\mathrm{p}-1)\ell}]$$

where the ith ℓ-symbol block of observables is given by

$$\boldsymbol{r}_{i\ell} \triangleq [r_{i\ell}, \ldots, r_{(i+1)\ell-1}] \quad i = 0, 1, 2, \ldots, n_\mathrm{p} - 1.$$

Similarly, we denote the ith disjoint block of corresponding transmitted symbols and estimated phases, respectively, as

$$\boldsymbol{x}_{i\ell} \triangleq [x_{i\ell}, \ldots, x_{(i+1)\ell-1}]$$
$$\hat{\boldsymbol{\theta}}_{i\ell} \triangleq [\hat{\theta}_{i\ell}, \ldots, \hat{\theta}_{(i+1)\ell-1}].$$

As previously mentioned, the estimated phase processes over the ℓ symbols of the ith block are kept constant, i.e. $\hat{\boldsymbol{\theta}}_{i\ell} = \hat{\theta}_{i\ell} \mathbf{1}_\ell$, where $\hat{\theta}_{i\ell}$ is a scalar and $\mathbf{1}_\ell$ denotes the length-ℓ vector with all elements equal to 1. In other words, the BW phase estimate for the kth sample, $k = 0, 1, 2, \ldots$, is equal to

$$\hat{\theta}_k = \hat{\theta}_{i\ell} \quad k = i\ell, i\ell + 1, \ldots, (i+1)\ell - 1.$$

Using the assumption of constant phase noise over a block, the MAP phase estimate on the ith block is

$$\hat{\theta}_{i\ell,\mathrm{MAP}} = \arg\max_{\vartheta \in [0,2\pi)} p(\vartheta|\boldsymbol{r}_{i\ell}) = \arg\max_{\vartheta \in [0,2\pi)} p(\boldsymbol{r}_{i\ell}|\vartheta)$$
$$= \arg\max_{\vartheta \in [0,2\pi)} \sum_{\boldsymbol{x}_{i\ell} \in \mathcal{X}^\ell} p(\boldsymbol{r}_{i\ell}|\vartheta, \boldsymbol{x}_{i\ell}) P(\boldsymbol{x}_{i\ell})$$

in which $p(\cdot|\cdot)$ denotes a conditional PDF and the last line is obtained marginalising with respect to the block of transmitted symbols and discarding the irrelevant ratio of a priori PDFs $p(\vartheta)/p(\boldsymbol{r}_{i\ell})$, since ϑ has a uniform marginal distribution over the interval $[0, 2\pi)$. Assuming the APP of the transmitted symbols is known, one can define the following modified APP-aided MAP phase estimate

$$\hat{\theta}_{i\ell} = \arg\max_{\vartheta \in [0,2\pi)} \sum_{\boldsymbol{x}_{i\ell} \in \mathcal{X}^\ell} p(\boldsymbol{r}_{i\ell}|\vartheta, \boldsymbol{x}_{i\ell}) P(\boldsymbol{x}_{i\ell}|\boldsymbol{r}) \quad (3)$$

where $\mathcal{X}^\ell$ denotes the set of length-ℓ sequences with elements drawn from the set $\mathcal{X}$ and $P(\boldsymbol{x}_{i\ell}|\boldsymbol{r})$ represents the APP of the transmitted symbols given the received block. According to the channel model (1), the conditional PDF $p(\boldsymbol{r}_{i\ell}|\vartheta, \boldsymbol{x}_{i\ell})$ is known and Gaussian. The term $P(\boldsymbol{x}_{i\ell}|\boldsymbol{r})$ can be easily computed from the bit log-likelihood ratios (LLRs) generated by the channel decoder for the considered modulation as described below.

Let us now define the following length-ℓ vector

$$\boldsymbol{\alpha}_k \triangleq [\alpha_k, \alpha_{k+1}, \ldots, \alpha_{k+\ell-1}]$$

where the generic element α_k, $k = 0, 1, \ldots$, is the *centre of gravity* of the transmitted constellation, obtained by weighting the possible symbol values by the corresponding APPs, at epoch k. Specifically, the vector $\boldsymbol{\alpha}_{i\ell}$ can be computed as

$$\boldsymbol{\alpha}_{i\ell} = \boldsymbol{P}_{i\ell} \tilde{\boldsymbol{x}}$$

where $\tilde{\boldsymbol{x}} = [\tilde{x}^{(0)}, \tilde{x}^{(1)}, \ldots, \tilde{x}^{(M-1)}]$ is the vector of constellation symbols and $\boldsymbol{P}_{i\ell}$ is an $\ell \times M$ matrix with elements

$$p_{lm} = P(\hat{x}_{i\ell+l} = \tilde{x}^{(m)}|\boldsymbol{r}) \quad (4)$$

in which $\hat{x}_{i\ell+l}$ is the hypothetical symbol at epoch $i\ell + l$, $l = 0, 1, \ldots, \ell - 1$, and $\tilde{x}^{(m)} \in \mathcal{X}$ is a symbol from the used constellation, $m = 0, 1, \ldots, M - 1$. In other words, p_{lm} is the APP that the symbol transmitted at time instant $i\ell + l$ is equal to the mth constellation symbol. Note that, if a constellation symbol $\tilde{x}^{(m)} \in \mathcal{X}$ has probability close to 1 at epoch $i\ell + l$, then $\alpha_{i\ell+l} \simeq \tilde{x}^{(m)}$. In particular, at time instants corresponding to pilot symbols, $\alpha_{i\ell+l} = x_{i\ell+l}$. On the other hand, if no APP is available, $\alpha_{i\ell+l}$ corresponds to the unweighted centre of the constellation.

The computation of the APPs p_{lm} in (4) can be performed in the following way. An M-ary symbol x_k is labelled by $b = \log_2 M$ bits $(c_k^{(1)}, \ldots, c_k^{(b)})$, $c_k^{(j)} \in \{0, 1\}$. Therefore, assuming that the bits in a given symbol are a posteriori independent, one can write

$$p_{lm} = \prod_{j=1}^{\log_2 M} P(c_{i\ell+l}^{(j)}|\boldsymbol{r}) = \prod_{j=1}^{\log_2 M} \frac{e^{\left(1 - c_{i\ell+l}^{(j)}\right)\mathcal{L}_{i\ell+l}^{(j)}}}{1 + e^{\mathcal{L}_{i\ell+l}^{(j)}}}$$

where

$$\mathcal{L}_{i\ell+l}^{(j)} \triangleq \ln \frac{P(c_{i\ell+l}^{(j)} = 0|\boldsymbol{r})}{P(c_{i\ell+l}^{(j)} = 1|\boldsymbol{r})} \quad j = 1, \ldots, \log_2 M$$

are the LLRs output either by the SISO channel decoder (coded bits) or by the SO demapper (free bits). The assumption of a-posteriori independence among these bits is expedient to the derivation of the iterative scheme. It may be reasonably verified for channel encoded bits, provided a sufficiently long pseudo-random LDPC code is used. On the other hand, this assumption may be critical for free (uncoded) bits unless proper interleaving is used. However, our numerical results show good performance, so this assumption will not be further discussed.

After straightforward manipulations, see, e.g. [27], the APP-based phase estimate for the kth symbol ($k = 0, 1, \ldots$) can be expressed as

$$\hat{\theta}_{k,\mathrm{BW}} = \arg\left[\boldsymbol{r}_{i\ell}(\boldsymbol{\alpha}_{i\ell})^\mathrm{H}\right] \quad k = i\ell, i\ell + 1, \ldots, (i+1)\ell - 1 \quad (5)$$

where the subscript BW has been introduced to specify the block-wise strategy and $(\cdot)^\mathrm{H}$ denotes the transpose complex conjugate, so that an inner product between vectors is considered.

3.2 Sliding window

As described in Section 3.1, the BW strategy is based on the use of disjoint consecutive ℓ-symbol windows. In this section, we extend the phase estimation to the use of an ℓ-symbol sliding window. Using the vector definitions given in Section 3.1, the BW-based strategy for a length-ℓ sliding window starting at epoch j can be written as

$$\hat{\theta}_{k,\mathrm{BW}} = \arg\left[\boldsymbol{r}_j(\boldsymbol{\alpha}_j)^\mathrm{H}\right] \quad k = j, j + 1, \ldots, j + \ell - 1$$

or, in scalar form, as

$$\hat{\theta}_{k,\mathrm{BW}} = \arg\left[\sum_{l=0}^{\ell-1} r_{j+\ell}\alpha_{j+\ell}^*\right] \quad k = j, j+1, \ldots, j+\ell-1$$

One can observe that a specific sample r_k at epoch k appears in ℓ overlapping windows, the first starting at epoch $k - \ell + 1$ and the last starting at epoch k. Therefore, the following phase estimate at the kth epoch can be heuristically considered

$$\hat{\theta}_{k,\mathrm{PLP}} = \arg\left[\sum_{l=0}^{\ell-1} \boldsymbol{r}_{k-l}(\boldsymbol{\alpha}_{k-l})^{\mathrm{H}}\right] \qquad (6)$$

where the subscript PLP will be shortly justified. The rationale behind (6) is to smooth the phase estimate (5) by averaging over all possible blocks which the kth sample belongs to. In the square brackets in (6), the term $r_k\alpha_k^*$ appears ℓ times, the terms $r_{k-1}\alpha_{k-1}^*$ and $r_{k+1}\alpha_{k+1}^*$ appear $\ell - 1$ times, the terms $r_{k-2}\alpha_{k-2}^*$ and $r_{k+2}\alpha_{k+2}^*$ appear $\ell - 2$ times and so on. Therefore, (6) can be also written, in scalar form, as

$$\hat{\theta}_{k,\mathrm{PLP}} = \arg\left[\sum_{j=-\ell+1}^{\ell-1} \pi_j r_{k-j}\alpha_{k-j}^*\right] \qquad (7)$$

where the following weights can be recognised

$$\pi_j = \ell - |j| \quad j = -\ell+1, \ldots, -1, 0, 1, \ldots, \ell-1.$$

The triangular *shape* of the coefficients $\{\pi_j\}$ in (7) is intuitively pleasing, since at the kth epoch the highest weight is assigned to the kth observable (associated with the kth transmitted symbol).

The phase estimation strategy (7) is a generalised (APP-based) instance of the PLP approach to phase estimation proposed in [16]. Therefore, we refer to this phase estimation strategy as APP-based PLP. An efficient implementation of (7) should rely on a shift register for the computation of (6). In fact, at the kth time instant, the shift register contains the terms $\boldsymbol{r}_{k-l}(\boldsymbol{\alpha}_{k-l})^{\mathrm{H}}$, $l = 0, \ldots, \ell - 1$; at epoch $k+1$, the new term $\boldsymbol{r}_{k+1}(\boldsymbol{\alpha}_{k+1})^{\mathrm{H}}$ is input and the 'oldest' term $\boldsymbol{r}_{k-\ell+1}(\boldsymbol{\alpha}_{k-\ell+1})^{\mathrm{H}}$ is dropped. The computational complexity of this implementation is discussed in Section 6.

4 Iterative receiver

The iterative receiver, shown as the right-most block in Fig. 1, is detailed in Fig. 2, in which dashed lines correspond to connections needed only in the presence of MLC, whereas concentric circles describe element-wise products between vectors.

The first operation at the receiver is a coarse phase pre-compensation of the received observables $\{r_k\}$ by means of an interpolator, which is based on the use of pilot symbols in the transmitted frame. We denote this phase estimate as $\hat{\varphi}_{\tilde{k}}$. Although various interpolation schemes with different performance can be designed, in this paper, we limit ourselves to a linear interpolation to minimise the system delay [28]. In particular, we use $N_{\mathrm{p}} = 1$ pilot symbol every N data symbols; therefore, if the $\tilde{k}$th epoch corresponds to a pilot symbol, then the next pilot symbols appear at time instants $\tilde{k} + N + 1$, $\tilde{k} + 2(N+1)$, $\tilde{k} + 3(N+1)$ and so on. At the positions of the pilot symbols, the phase noise is estimated as the difference between the phase of the received sample and the phase of the transmitted pilot symbol

$$\hat{\varphi}_{\tilde{k}} = \angle r_{\tilde{k}} x_{\tilde{k}}^*. \qquad (8)$$

Note that this estimation is asymptotically exact at high SNR; in fact, in the high-SNR regime $r_{\tilde{k}} \simeq x_{\tilde{k}} e^{j\theta_{\tilde{k}}}$ and, therefore, $\hat{\varphi}_{\tilde{k}} \simeq \theta_{\tilde{k}}$. The phase noise affecting the intermediate data symbols is pre-estimated by linearly interpolating two consecutive phase estimates $\hat{\varphi}_{\tilde{k}}$ and $\hat{\varphi}_{\tilde{k}+N+1}$ to obtain $\hat{\varphi}_k$. In particular, the kth data symbol is located between two pilot symbols at positions $\lfloor k/N \rfloor$ and $\lfloor k/(N+1) \rfloor$, respectively, where $\lfloor x \rfloor$ denotes the largest integer smaller than or equal to x. Therefore, the phase estimate at epoch k can be written as

$$\hat{\varphi}_k = \hat{\varphi}_{\lfloor k/N \rfloor} + \left(\hat{\varphi}_{\lfloor k/(N+1) \rfloor} - \hat{\varphi}_{\lfloor k/N \rfloor}\right)\left(k - \left\lfloor \frac{k}{N} \right\rfloor\right)\frac{1}{N+1}$$
$$= \hat{\varphi}_{\lfloor k/N \rfloor} + \left(\hat{\varphi}_{\lfloor k/(N+1) \rfloor} - \hat{\varphi}_{\lfloor k/N \rfloor}\right)\frac{k \bmod (N+1)}{N+1}.$$

The use of pre-compensation is expedient to perform the first demodulation/decoding act, which is required to perform APP-based phase estimation. The observable at the output of the pre-compensation block, denoted as $\tilde{r}_k$, is obtained as a derotation by $\hat{\varphi}_{\tilde{k}}$ of the observable r_k and can be expressed as

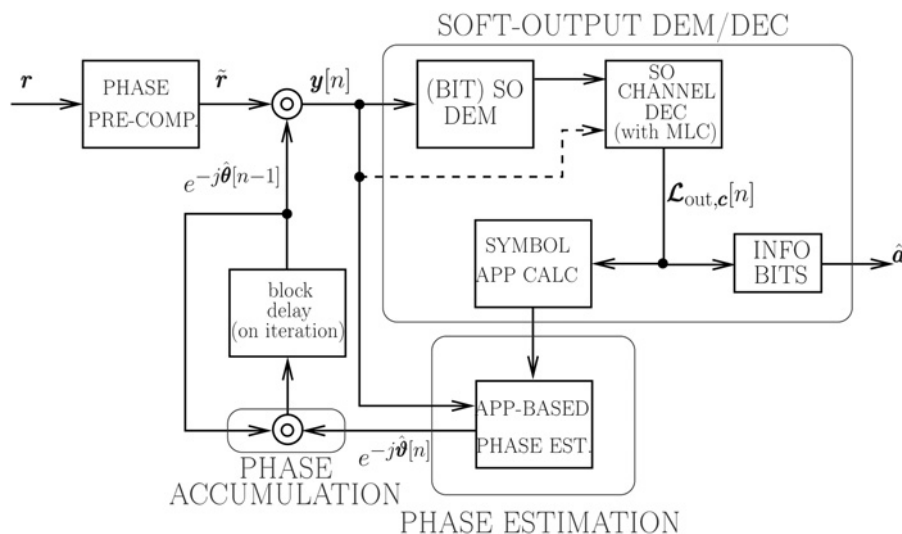$$\tilde{r}_k = r_k e^{-j\hat{\varphi}_k} = x_k e^{j(\theta_k - \hat{\varphi}_k)} + \tilde{n}_k \qquad (9)$$

Fig. 2 *Block diagram of the proposed iterative receiver. The dashed line is used only with MLC*

where $\{\tilde{n}_k\}$ are still i.i.d. Gaussian samples with the same variance of $\{n_k\}$. The phase noise $\{\theta_k - \hat{\varphi}_k\}$ affecting $\{\tilde{r}_k\}$ may have a different statistical characterisation with respect to $\{\theta_k\}$. However, since the proposed APP-based synchronisation algorithms (namely, BW and PLP) require very limited a priori statistical characterisation of the phase noise, they can still be applied directly and a more accurate statistical characterisation of the phase noise after pre-compensation is not required.

The observables $\{\tilde{r}_k\}$ at the output of the pre-compensation block feed the input of the SISO QAM demodulator. We consider a simplified demodulator version for which the approximate LLRs associated with the kth observable output by the demodulator can be written as [29]

$$\mathcal{L}(c_k^{(j)}|r_k) = -\frac{1}{2\sigma^2}\left[\min_{x_k \in \mathcal{X}_0^{(j)}}|\tilde{r}_k - x_k|^2 - \min_{x_k \in \mathcal{X}_1^{(j)}}|\tilde{r}_k - x_k|^2\right] \quad (10)$$

where $\mathcal{X}^{(j)}$ denotes the set of QAM symbols with bit $c_k^{(j)}$ in position j, $j = 1, 2, \ldots, \log_2 M$, and the following max-log approximation for sufficiently large SNR has been used [30]

$$\ln \sum_u e^{f(u)} \simeq \max_u f(u)$$

in which u belongs to a discrete set and $f(u)$ is a given function of u. These soft values are used in a SISO decoder which outputs the LLRs on the multi-level coded bits. We now detail the structure of the (multi-level) SISO decoder.

Off-the-shelf channel decoding, e.g. message passing for LDPC codes with *internal* decoding iterations, is performed for small constellations where all bits are channel encoded. For large constellations, where part of the bits is channel encoded and part is left uncoded, multi-stage decoding [18] is performed. In particular, the soft outputs on the b_1 coded bits output by the LDPC decoder are used to compute the APP of each b_1-bit subset, denoted as $\mathcal{S}_k^{(s)}$, as

$$P(\mathcal{S}_k^{(s)}) = \prod_{m=1}^{b_1} P(c_k^{(j)} = \mathcal{C}_m^{(s)}) \quad s = 1, \ldots, 2^{b_1}$$

where $\mathcal{C}_m^{(s)}$ is the value of the mth bit in the label associated with the sth subset and, to simplify the notation, conditioning on the received signal and dependence on the iteration index are here understood. By using the total probability theorem, one obtains the APPs of the free bits $f_k^{(j)}$ associated with the kth symbol in terms of the subset APPs as

$$P(f_k^{(i)}) = \sum_{s=1}^{2^{b_1}} P(f_k^{(i)}|\mathcal{S}_k^{(s)})P(\mathcal{S}_k^{(s)}) \quad (11)$$

where the APPs $P(f_k^{(i)}|\mathcal{S}_k^{(s)})$ over the QAM subset $\mathcal{S}_k^{(s)}$ can be computed in terms of subset LLRs similar to those described in (10). The computational complexity of (11) can be reduced by observing that there are typically a few subsets, namely B, with higher probability and neglecting the contribution from less likely subsets. Considering only the retained subsets, the APPs on the free bits can be therefore computed as

$$P(f_k^{(i)}) = \frac{1}{\sum_{s'=1}^{B} P(\mathcal{S}_k^{(s')})} \sum_{s=1}^{B} P(f_k^{(i)}|\mathcal{S}_k^{(s)})P(\mathcal{S}_k^{(s)})$$

where the factor $1/\sum_{s'=1}^{B} P(\mathcal{S}_k^{(s')})$ is needed for correct normalisation. Results, not reported here for conciseness, show that taking into account the sole most likely subset, i.e. using $B = 1$, leads to minor performance degradation and a significant complexity saving. According to this reduced-complexity approximation with $B = 1$, hard decisions on the code bits are

considered to select the most likely subset of size 2^{b-b_1}, so that the APPs of the free bits are then computed restricting (10) to this selected subset.

The LLRs of the (multi-level) coded bits are combined to generate APPs on the constellation symbols, which in turn are passed to the phase synchronisation block. The cascade of phase estimation and demodulation/decoding steps is referred to as an *external* iteration and n_{it} denotes its maximum number. The 0th iteration, corresponding to $n = 0$, refers to a first detection/decoding act on the observables $\tilde{r}_k$ at the output of the pre-compensation block. The LLRs for all symbols in a codeword are collected in the vector $\mathcal{L}_{\text{out},c}[n]$, where n denotes the external iteration index.

The iterative algorithm can now be summarised as follows (see Fig. 2). Let us define the vectors $\boldsymbol{y}[n]$, $\tilde{\boldsymbol{r}}$ and $\hat{\boldsymbol{\theta}}[n-1]$, by analogy with vector $\boldsymbol{r}$, as the collection of the corresponding samples within a codeword at the indicated iteration. At the nth iteration, $n = 1, \ldots, n_{\text{it}}$, APP-based synchronisation is performed based on the observable vector $\boldsymbol{y}[n]$, which is given by

$$\boldsymbol{y}[n] = \tilde{\boldsymbol{r}} \circ e^{-j\hat{\boldsymbol{\theta}}[n-1]} \quad (12)$$

where $\hat{\boldsymbol{\theta}}[0] = \mathbf{0}$, $\circ$ denotes an element-wise vector product, and the exponential is applied element-wise to the vector $\hat{\boldsymbol{\theta}}[n-1]$. The observable $\boldsymbol{y}[n]$ is used in the demapping/decoding blocks to compute the symbol APPs needed by (5) or (6) for BW or PLP phase estimation, respectively. Since $\boldsymbol{y}[n]$ is a derotated version, at each iteration, of the observable $\tilde{\boldsymbol{r}}$, the phase estimate output by the APP-based synchroniser corresponds to a residual phase error $\hat{\boldsymbol{\vartheta}}[n]$, which must be accumulated to obtain the overall phase estimate in (12)

$$\hat{\boldsymbol{\theta}}[n] = \hat{\boldsymbol{\theta}}[n-1] + \hat{\boldsymbol{\vartheta}}[n]. \quad (13)$$

The final hard decision on the transmitted information bits in a codeword, denoted as $\hat{\boldsymbol{a}}$, is made at the end of the n_{it}th external iteration.

5 Performance analysis

We investigate the BER performance of the proposed receiver schemes with iterative synchronisation and demodulation/decoding for an LDPC-coded QAM scheme according to the simulation set-up summarised in Table 1.

We first investigate the impact of the window length ℓ on the system performance. In Fig. 3, the BER is shown, as a function of ℓ, considering a scheme with 64-QAM, $n_{\text{it}} = 5$ external iterations, pilot spacing $N = 50$ and various values of γ_b (12.1 and 12.7 dB) and σ_Δ (0.51° and 1°). Both BW and PLP estimation algorithms are considered. From the results in Fig. 3, a compromise value of ℓ can be selected in order to minimise the BER, as discussed at the beginning of Section 3. In particular, $\ell = 24$ is a good window

Table 1 Simulation set-up

| Parameter	Value
pilot constellation	4-QAM constellation with energy $E_p = 2.5E_s$
MLC scheme	$b_1 = 4$
LDPC code rate	$R = \frac{k}{n} = \frac{7056}{8064} = \frac{7}{8}$
type of LDPC code	Compliant with the exponent parity-check matrix structure described in the WiMAX standard [31, Paragraph ~ 8.4.9.2.5, Annex H]: $n_{b,r} = 12$ rows, $n_{b,c} = 96$ columns, spreading factor $Z_f = 84$ constant row weight $w_r = 32$ and average column weight $w_c = 4$
maximum number of LDPC internal iterations	50 (our results show that, if BER < 10^{-2}, 5 internal iterations are sufficient)
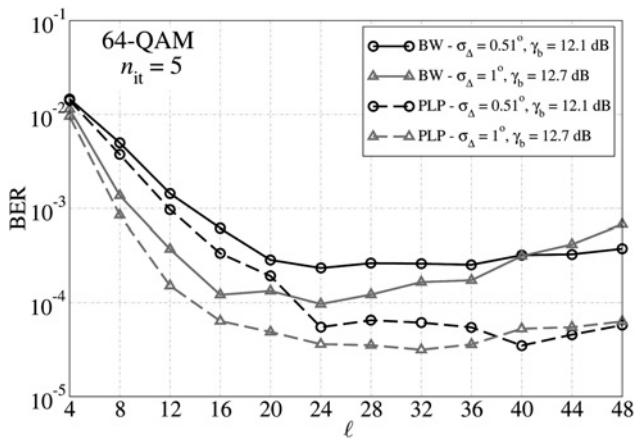
Fig. 3 *BER, as a function of ℓ, considering a 64-QAM, $n_{it} = 5$ external iterations, pilot spacing $N = 50$ and various values of γ_b and σ_Δ. Both BW and PLP phase estimation strategies are considered*

length with the BW phase estimation strategy, for all considered values of γ_b and σ_Δ. With the PLP phase estimation strategy the performance improves, since the lowest achievable BER is lower than that relative to the BW case. In general, $\ell = 32$ guarantees approximately a good performance in all the considered PLP cases. Further results (not reported here for brevity) show that
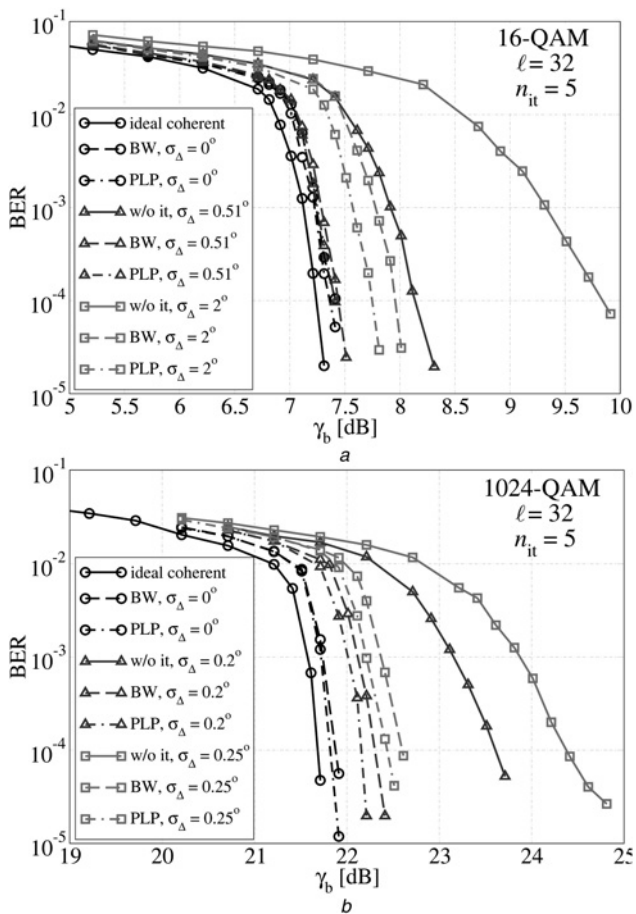

Fig. 4 *BER, as a function of γ_b, considering $n_{it} = 5$ external iterations, $\ell = 32$, pilot spacing $N = 50$ and various values of σ_Δ. The performance of BW and PLP are compared for*

a 16-QAM
b 1024-QAM

good performance can be achieved with $\ell = 32$ and various systems settings, i.e. small or large constellation sizes, mild or strong phase noise and BW or PLP phase estimation. This means that $\ell = 32$ can be used in all considered scenarios demonstrating the proposed algorithms require very limited a priori knowledge on the phase noise statistics.

In Fig. 4, the BER is shown, as a function of γ_b, considering $n_{it} = 5$ external iterations, $\ell = 32$, pilot spacing $N = 50$ and various values of σ_Δ. The performance of systems embedding BW and PLP strategies is compared for two modulation formats: (Fig. 4a) 16-QAM and (Fig. 4b) 1024-QAM. As a reference, in both figures we also show the performance without iterations, i.e. in the case where, after interpolation, demodulation and decoding are carried out just once. For $\sigma_\Delta = 0°$, due to the residual noise introduced by interpolator and phase estimator one can observe a small performance loss – on the order of $0.15 \div 0.2$ dB – with respect to an ideal coherent system which is fed with exact phase information and does not use interpolation and synchronisation. As expected, the higher the phase noise intensity, the worse the performance; the larger the constellation size, the lower the robustness against phase noise. For strong phase noise intensity, the performance improvement brought by the PLP phase estimation strategy, with respect to the BW strategy, is more evident. The performance of the proposed iterative receivers may improve when the number of external iterations increases. However, other simulation results (not shown here for brevity) indicate that increasing the number of iterations from 3 to 5 leads to a remarkable performance improvement, whereas increasing them from 5 to 10 leads to negligible further advantages.

In Fig. 5, the BER is shown, as a function of γ_b, for 1024-QAM, $\sigma_\Delta = 0.21°$, $n_{it} = 5$ external iterations, pilot spacing $N = 48$ and window length $\ell = 32$. The performance of the proposed iterative schemes (with BW and PLP phase estimation strategies) is compared with the performance of the joint iterative receiver proposed in [15], referred to as 'joint MAP,' operating on *r*. As expected, the best performance is obtained by the reference joint MAP scheme, but the PLP approach exhibits only a 0.1 dB loss. Further results, not shown here for shortness, show that the PLP-based approach is more robust for large constellation sizes, due to the fact that the relative loss, with respect to the joint MAP scheme, decreases with the constellation size. Moreover, the joint MAP approach of [15] requires the design of a proper factor graph for the iterative receiver and knowledge of the phase noise intensity. Finally, note that the considered value of $\sigma_\Delta = 0.21°$ is remarkable, if compared with 1.85°, which is approximately half the minimum phase difference between 1024-QAM constellation points having the same energy.
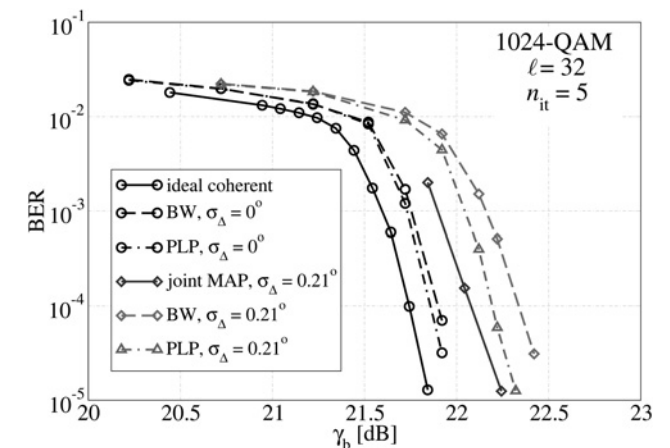

Fig. 5 *BER, as a function of γ_b, of the proposed BW and PLP approaches compared with joint MAP in [15] for 1024-QAM, for $\sigma_\Delta = 0.21°$, $n_{it} = 5$ external iterations, pilot spacing $N = 48$ and $\ell = 32$*

Table 2 Number of elementary operations per modulated symbol and external iteration required for synchronisation by BW, PLP and joint MAP algorithms

	BW	PLP	JointMAP
real additions	$\left[\dfrac{2\log_2 M}{n}\left(\dfrac{\log_2 M}{nN}\right)+\dfrac{1}{N}+3\right]\dfrac{1}{n_{\text{it}}+1}$ $+\left(2M+2+2\dfrac{\ell-1}{\ell}\right)\dfrac{n_{\text{it}}}{n_{\text{it}}+1}+3M$	$\left[\dfrac{2\log_2 M}{n}\left(\dfrac{\log_2 M}{nN}\right)+\dfrac{1}{N}+3\right]\dfrac{1}{n_{\text{it}}+1}$ $+(2M+8)\dfrac{n_{\text{it}}}{n_{\text{it}}+1}+3M$	$8+M(11+\log_2 M)$
real multiplications	$\left[\dfrac{4\log_2 M}{n}\left(\dfrac{\log_2 M}{nN}\right)+4\right]\dfrac{1}{n_{\text{it}}+1}+(2M+8)\dfrac{n_{\text{it}}}{n_{\text{it}}+1}+3M$		$8+18M$
real divisions	$\dfrac{1}{N}\dfrac{1}{n_{\text{it}}+1}$		$6+M$
exponentials	–		$2M$
absolute values	–		$2+M$
square roots	–		M
logarithms	–		$\log_2 M$
Arg functions	$\left(\dfrac{1}{N}+\dfrac{\log_2 M}{n}\right)\dfrac{1}{n_{\text{it}}+1}+\dfrac{n_{\text{it}}}{n_{\text{it}}+1}$		–
minimum	$2\log_2 M$		–

6 Computational complexity

In this section, we compare the computational complexity of the proposed iterative synchronisation and decoding algorithms with that of the joint MAP scheme. All algorithms are based on successive (external) iterations between two main functional operations: (i) phase synchronisation and (ii) SISO decoding, in which the symbol APPs are computed by exploiting the selected error correction code. In this paper, we only focus on the first task, since the computational burden related to the decoding block of the LDPC code is common to all the algorithms. The computational complexity is defined as the number of real multiplications and additions per modulated symbol and external iteration. Note that one complex multiplication requires four real multiplications and two real additions.

The computational complexity of the proposed synchronisation algorithm can be summarised as follows:

(i) The first computations, carried out by the interpolator, correspond to (8) and (9). Denoting as K the codeword length, this step requires: $4/N+4/K+4$ real multiplications, $3/N+2/K+3$ real additions, $1/N$ real divisions and $1/N+1/K$ argument functions.
(ii) At each iteration, two operations are performed: (i) generation of the LLRs to be input to the channel decoder and (ii) phase estimation [i.e. (5) for BW or (6) for PLP]. The former requires: $3M$ real multiplications, $3M$ real additions and $2\log_2 M$ minimum functions. The latter, instead, requires: $2M+8$ real multiplications, 1 argument function and $2M+2+2(\ell-1)/\ell$ or $2M+8$ real additions for BW or PLP, respectively.

Therefore, this analysis shows that the number of multiplications and additions grows asymptotically with $5M$ (for large M) for both BW and PLP estimation strategies.

The joint MAP algorithm involves the following computational steps:

(i) First, coefficients for graph-based phase estimation are evaluated for each codeword symbol using [15, eqs. (15)–(17)]. This step requires: $5M+6$ real multiplications, $4M+2$ real additions and 2 real divisions.
(ii) Then, forward and backward parameters are updated using [15, eqs. (20)–(21)]. This step requires: 2 real multiplications, 6 real additions, 4 real divisions and 2 modulus functions.
(iii) APPs are generated using [15, eq. (22)]. This step requires: $13M$ real multiplications, $7M$ real additions, M real divisions, M modulus functions, M square roots and $2M$ exponentials.
(iv) Finally, input LLRs are generated, using standard methods, employing $M\log_2 M$ real additions and $\log_2 M$ logarithms.

Therefore, the joint MAP algorithm entails numbers of multiplications and additions equal to $8+18\,M$ and $8+M(11+\log_2 M)$, respectively. We remark that the computational complexity of the joint MAP approach, here derived independently, is compliant with that given in [32, Table I]. The number of elementary operations per modulated symbol and external iteration required by the synchronisation function for BW, PLP and joint MAP algorithms are detailed in Table 2.

On the basis of the evaluation outlined above, one can define the normalised computational load of the proposed algorithms as the following ratios between the number of multiplications (additions) required by the proposed solutions and the corresponding ones required by joint MAP

$$\xi_{\text{M}} \triangleq \frac{\text{Number of multiplications in BW or PLP}}{\text{Number of multiplications in [15]}}$$

$$\xi_{\text{A}} \triangleq \frac{\text{Number of additions in BW or PLP}}{\text{Number of additions in [15]}}.$$

The relative computational loads ξ_{M} and ξ_{A} can be computed on the basis of Table 2. The resulting values are shown, as functions of M, in Fig. 6. It can be observed that ξ_{M} and ξ_{A} are always less than one, i.e. BW and PLP have a computational complexity lower than that of the joint MAP algorithm. Moreover, the overall computational loads of the proposed solutions, with respect to [15], are decreasing functions of the constellation size. In particular, ξ_{M} saturates for large constellation sizes, say $M \geq 64$, whereas ξ_{A} keeps on
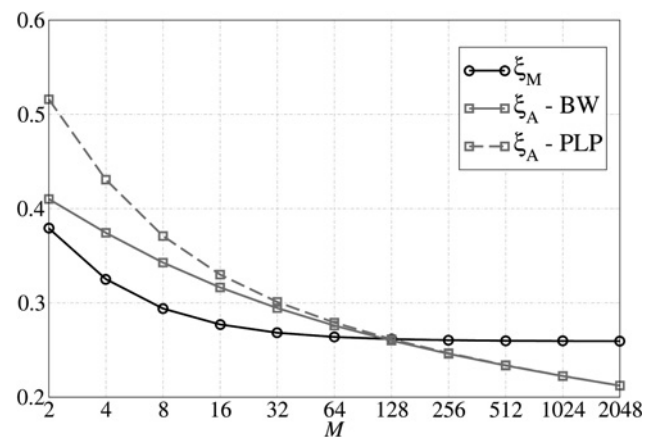

Fig. 6 *Normalised computational loads of the proposed synchronisation algorithms, as functions of M, for the considered simulation settings*

decreasing. Therefore, both BW and PLP approaches have a significantly lower computational complexity, with respect to the joint MAP approach, for medium–high constellation sizes, yet incurring a minor performance loss as discussed in the previous Section 5.

7 Concluding remarks

This paper presents low-complexity MAP phase estimation algorithms which may operate effectively with very limited statistical knowledge of the channel phase noise process. These algorithms can be employed in an iterative receiver with separate synchronisation and decoding. In particular, two estimation strategies are considered. First, under the assumption of constant phase noise over a sufficiently short interval, a BW strategy is presented. Then, an improved PLP phase estimation strategy, which encompasses the presence of a sliding window to smooth the piecewise phase estimate of the BW approach is proposed. The results with pilot-aided LDPC-coded QAMs show that the PLP solution guarantees a good performance for medium–high constellation sizes and challenging phase noise scenarios, also with respect to the benchmark joint approach. The proposed solutions are particularly attractive from the implementation viewpoint for spectrally efficient communications employing high-order modulations, due to their low computational complexity and pragmatic nature which allows the use of off-the-shelf detection and decoding subblocks.

8 References

1 Rutman, J., Walls, F.: 'Characterization of frequency stability in precision frequency sources', *Proc. IEEE*, 1991, **79**, (7), pp. 952–960
2 Barbieri, A., Colavolpe, G.: 'On the information rate and repeat-accumulate code design for phase noise channels', *IEEE Trans. Commun.*, 2011, **59**, (12), pp. 3223–3228
3 Barletta, L., Magarini, M., Spalvieri, A.: 'The information rate transferred through the discrete-time Wiener's phase noise channel', *J. Lightwave Technol.*, 2012, **30**, (10), pp. 1480–1486
4 Martalò, M., Tripodi, C., Raheli, R.: 'On the information rate of phase noise-limited communications'. Information Theory and Applications Workshop (ITA), San Diego, CA, USA, February 2013, pp. 1–7
5 Ghozlan, H., Kramer, G.: 'Multi-sample receivers increase information rates for Wiener phase noise channels'. Proc. IEEE Global Telecommunication Conf. (GLOBECOM), Atlanta, GA, USA, December 2013, pp. 1897–1902
6 Lehmann, F., Kazem, A., Salut, G.: 'Blind turbo-detection in the presence of phase noise', *IET Commun.*, 2009, **3**, (8), pp. 1343–1353
7 Herzet, C., Noels, N., Lottici, V., *et al*.: 'Code-aided turbo synchronization', *Proc. IEEE*, 2007, **95**, (6), pp. 1255–1271
8 Noels, N., Steendam, H., Moeneclaey, M.: 'Performance analysis of ML-based feedback carrier phase synchronizers for coded signals', *IEEE Trans. Signal Process.*, 2007, **55**, (3), pp. 1129–1136
9 Wu, N., Wang, H., Li, Z., *et al*.: 'Performance analysis of code-aided iterative carrier phase recovery in turbo receivers', *IET Commun.*, 2012, **6**, (17), pp. 2980–2988
10 Wu, X., Xiang, H.: 'Iterative carrier phase recovery methods in turbo receivers', *IEEE Commun. Lett.*, 2005, **9**, (8), pp. 735–737
11 Nissila, M., Pasupathy, S.: 'Adaptive iterative detectors for phase-uncertain channels via variational bounding', *IEEE Trans. Commun.*, 2009, **57**, (3), pp. 716–725
12 Krishnan, R., Khanzadi, M.R., Eriksson, T., *et al*.: 'Soft metrics and their performance analysis for optimal data detection in the presence of strong oscillator phase noise', *IEEE Trans. Commun.*, 2013, **61**, (6), pp. 2385–2395
13 Lehmann, F.: 'A Gaussian sum approach to blind carrier phase estimation and data detection in turbo coded transmissions', *IEEE Trans. Commun.*, 2009, **57**, (9), pp. 2619–2632
14 Benvenuto, L., Giugno, L., Lottici, V., *et al*.: 'Code-aware carrier phase noise compensation on turbo-coded spectrally-efficient high-order modulations'. Proc. Int. Workshop Signal Processing for Space Communications (SPSC), Catania, Italy, September 2003, pp. 1–8
15 Barbieri, A., Colavolpe, G., Caire, G.: 'Joint iterative detection and decoding in the presence of phase noise and frequency offset', *IEEE Trans. Commun.*, 2007, **55**, (1), pp. 171–179
16 Ferrari, G., Colavolpe, G., Raheli, R.: 'On linear predictive detection for communications with phase noise and frequency offset', *IEEE Trans. Veh. Technol.*, 2007, **56**, (4), pp. 2073–2085
17 Martalò, M., Ferrari, G., Asim, M., *et al*.: 'Reducedcomplexity synchronization for high-order coded modulations'. Proc. IEEE Int. Conf. on Communication (ICC), London, UK, June 2015, pp. 4721–4726
18 Wachsmann, U., Fischer, R.F.H., Huber, J.B.: 'Multilevel codes: theoretical concepts and practical design rules', *IEEE Trans. Inf. Theory*, 1999, **45**, (5), pp. 1361–1391
19 Li, Y., Ryan, W.E.: 'Bit-reliability mapping in LDPC-coded modulation systems', *IEEE Commun. Lett.*, 2005, **9**, (1), pp. 1–3
20 Wesel, R.D., Liu, X., Cioffi, J.M., *et al*.: 'Constellation labeling for linear encoders', *IEEE Trans. Inf. Theory*, 2001, **47**, (6), pp. 2417–2431
21 Proakis, J.G.: 'Digital communications' (McGraw-Hill, New York, NY, USA, 2001, 4th edn.)
22 Cavers, J.K.: 'An analysis of pilot symbol assisted modulation for Rayleigh fading channels', *IEEE Trans. Veh. Technol.*, 1991, **40**, (4), pp. 686–693
23 Ferrari, G., Anastasopoulos, A., Colavolpe, G., *et al*.: 'Adaptive iterative detection for the phase-uncertain channel: limited-tree-search versus truncated-memory detection', *IEEE Trans. Veh. Technol.*, 2004, **53**, (2), pp. 433–442
24 Demir, A., Mehrotra, A., Roychowdhury, J.: 'Phase noise in oscillators: a unifying theory and numerical methods for characterization', *IEEE Tran. Circuits Syst. I, Fundam. Theory Appl.*, 2000, **47**, (5), pp. 655–674
25 Kasdin, N.J.: 'Discrete simulation of colored noise and stochastic processes and $1 = (f^\alpha)$ power law noise generation', *Proc. IEEE*, 1995, **83**, (5), pp. 802–827
26 Khanzadi, M.R., Mehrpouyan, H., Alpman, E., *et al*.: 'On models, bounds, and estimation algorithms for time-varying phase noise'. IEEE Int. Conf. Signal Processing and Communication Systems (ICSPCS), Honolulu, HI, USA, December 2011, pp. 1–8
27 Lottici, V., Luise, M.: 'Embedding carrier phase recovery into iterative decoding of turbo-coded linear modulations', *IEEE Trans. Commun.*, 2004, **52**, (4), pp. 661–669
28 Torrance, J.M., Hanzo, L.: 'Comparative study of pilot symbol assisted modem schemes'. Proc. Int. Conf. Radio Receivers and Associated Systems, Bath, UK, September 1995, pp. 36–41
29 Viterbi, A.J.: 'An intuitive justification and a simplified implementation of the MAP decoder for convolutional codes', *IEEE J. Select. Areas Commun.*, 1998, **16**, (2), pp. 260–264
30 Anastasopoulos, A., Chugg, K.M., Colavolpe, G., *et al*.: 'Iterative detection for channels with memory', *Proc. IEEE*, 2007, **95**, (6), pp. 1272–1294
31 'Approved Draft IEEE Standard for Local and metropolitan area networks Corrigendum to IEEE Standard for Local and Metropolitan Area Networks-Part 16: Air Interface for Fixed Broadband Wireless Access Systems (Incorporated into IEEE Std 802.16e-2005 and IEEE Std 802.16-2004/Cor 1-2005 E)', *IEEE Std P802.16/Cor1/D5*, 2005
32 Shayovitz, S., Raphaeli, D.: 'Efficient iterative decoding of LDPC in the presence of strong phase noise'. Proc. Int. Symp. on Turbo Codes & Related Topics, Gothenburg, Sweden, August 2012, pp. 1–5